Earth and Planetary Science Letters 297 (2010) 453–460

Contents lists available at ScienceDirect

Earth and Planetary Science Letters

journal homepage: www.elsevier.com/locate/epsl

Age and Prematurity of the Alps Derived from Topography

S. Hergarten *, T. Wagner, K. Stüwe

Institute of Earth Sciences, University of Graz, Austria

ARTICLE INFO

Article history:
Received 29 March 2010
Received in revised form 25 June 2010
Accepted 29 June 2010
Available online 31 July 2010

Editor: T.M. Harrison

Keywords:
Alps
topography
erosion
slope
denudation

ABSTRACT

The European Alps are one of the best studied mountain ranges on Earth, but yet the age of their topography is almost unknown. Even their relative stage of evolution is unclear: Are the Alps still growing, in a steady state or already decaying, and is there a significant difference between Western and Eastern Alps? Using a new geomorphic parameter we analyze the topography of the Alps and provide one of the first quantitative constraints demonstrating that the range is still in its infancy: In contrast to several other mountain ranges, the Alps have still more than half of their evolution to a geomorphic steady state to go. Combining our results with sediment budget data from the surrounding basins we infer that the formation of the present topography began only 5-6 million years ago. Our results question the apparent consensus that the topographic evolution is distributed over much of the Miocene and might give new impulses to the reconstruction of paleoclimate in Central Europe.

1. Introduction

Geologically, the European Alps are among the best studied mountain ranges on Earth. Curiously, one of the least understood aspects of the range is the very age of its topography. While the structural frame of the present topography evolved in early to middle Miocene (Frisch et al., 1998), even the huge amount of available data seems not to be sufficient for deciphering the history of the Alpine topography. Even their stage of maturity seems to be unclear: Are the Alps still growing, in a steady state or already decaying?

Low-temperature geochronological data – both from detrital record (Dunkl and Frisch, 2002) and from crystalline basement (Vernon et al., 2006, 2008; Luth and Willingshofer, 2008) – constitute a large part of the available data. From these data, mean exhumation rates can be derived, documenting considerable erosion during the Miocene. Sediment budgets from the sedimentary basins around the Alps (Kuhlemann et al., 2001) point towards the same direction, but beyond this, they indicate a sudden rise of sediment supply some five million years ago which has not been explained yet. Even more important, the relationship of exhumation to topography development is in general questionable (Stüwe and Barr, 1998). Topographic change reflects the difference between rock uplift and denudation, and both can hardly be measured on the same time scale.

Erosion history carries some more puzzles such as the Augenstein surfaces on the karst plateaus of the Eastern Alps (Frisch et al., 2001). These and other paleosurfaces from the Eocene indicate very low erosion rates locally (Hejl, 1997).

Drainage patterns also play an important part in the evolution of mountain belts (e.g, Schlunegger and Hinderer, 2001; Robl et al., 2008a,b). However, although they often reveal information on relative base level lowering, they seem not to be suitable for deriving the history of topography.

Several studies based on fossil records provide direct evidence for a high and locally steep relief in and even before the Miocene (e.g., Kocsis et al., 2007). However, we should keep in mind that these results are always local and limited to a few points on the time axis, so that they may only put some constraints on the history of topography. Furthermore, these data are associated with a considerable uncertainty on a quantitative level as demonstrated by Hay et al. (2002).

In sum, the age of formation of the Alpine mountain range remains poorly understood. Even for the present day regime there is only a sketchy understanding about the current uplift and erosion rates: Geodetic measurements of uplift rates were published for the Central Alps (Kahle, 1997) and for the Eastern Alps (Ruess and Höggerl, 2002), and some measurements of Holocene erosion rates exist (von Blanckenburg et al., 2007; Wittmann et al., 2007; Norton et al., 2010b), but the present day relationship of uplift and erosion or their drivers remains speculative. For the Western Central Alps a pattern arises that suggests that much of the present day uplift is due to isostatic rebound and that the tectonically driven uplift has terminated (Barletta et al., 2006; Champagnac et al., 2007). This is supported by first data that appear to indicate that there is a direct correlation of erosion rate with elevation and with uplift rate (Wittmann et al., 2007; Champagnac et al., 2009). However such

* Corresponding author. Tel.: +43 316 3805594.
E-mail addresses: stefan.hergarten@uni-graz.at (S. Hergarten), thomas.wagner@uni-graz.at (T. Wagner), kurt.stuewe@uni-graz.at (K. Stüwe).

0012-821X/$ – see front matter © 2010 Elsevier B.V. All rights reserved.
doi:10.1016/j.epsl.2010.06.048

information is still in its infancy and usually confined to small areas studied in much detail.

2. The Peculiar Topography of the Alps

River profiles become steeper with increasing elevation and slopes show the same tendency in the mean. The straightforward explanation of this phenomenon hinges on the concept of geomorphic equilibrium: Under temporally constant conditions, the land surface evolves towards a steady state where erosion balances rock uplift. As fluvial erosion increases with both slope and catchment size, the smaller catchment sizes found at high elevations must be compensated by steeper slopes in case of spatially uniform rock uplift (Whipple and Tucker, 1999; Wobus et al., 2006). So an increase of slopes with elevation should be expected. If the influence of the catchment size can be eliminated, slopes reveal information on recent erosion rates and, in case of equilibrium, on uplift rates.

This idea is not limited to the case of homogeneous uplift. In mountain belts, rock uplift is in fact often inhomogeneously distributed and tends to increase from the margins toward the crest. Thus, high elevations are often a result of high rock uplift rates and therefore erosion rates should increase with elevation too. For the Alps, this is directly confirmed by measurements of recent uplift rates (e.g., Kahle, 1997) and estimates of erosion rates from cosmogenic nuclei (e.g., Wittmann et al., 2007). Therefore, both decreasing catchment sizes and heterogeneous uplift should lead to a rather strong increase of slopes with elevation. As stated above, deriving erosion rates from slopes requires the elimination of the effect of different catchment sizes. In the so called stream power approach (Whipple and Tucker, 1999; Wobus et al., 2006), this is done by assuming a power-law dependence of the erosion rate on the catchment size. However, as there is still uncertainty about the exponent, we try another approach that avoids the comparison of catchments of different sizes: We compare slopes at different elevations over the entire mountain range, but use only slopes of points in the digital elevation model (DEM) that have approximately the same catchment size. In the following, $\overline{S}_A$ denotes the average slope of all surface points with catchment size close to A. As long as the considered area contains a sufficient amount of points with catchment size A, $\overline{S}_A$ provides a reasonable proxy for the recent erosion rate.

In the following we apply this idea to the topography of the Alps using the freely available SRTM3 DEM. Regions without runoff were filled in order to get consistent catchment sizes, but all points where the elevation had to be increased were excluded from the analysis since filling affects the slopes. For our purpose we define the study area as the connected region of the Alps above 600 m elevation as shown in Fig. 1.

Fig. 2 displays the obtained relationship between $\overline{S}_A$ and elevation for various catchment sizes. The data were averaged with a moving window of 100 m size in elevation, while catchment sizes were subdivided into logarithmic classes. For all considered catchment sizes in the range shown, we find the expected strong increase of $\overline{S}_A$ with elevation only up to about 1500-2000 m. Excitingly, $\overline{S}_A$ decreases again above this elevation for all considered catchment sizes except for the smallest class.

Qualitatively, this finding is not new. Kühni and Pfiffner (2001) found that the increase of mean slope with elevation ceases at about 1600 m in the Swiss Alps. However, they averaged slope values over various catchment sizes and thus found no decrease with elevation. Fitzsimons and Veit (2001) speak of "relatively flat surfaces at higher elevations, especially in the alpine altitudinal belt". The occurrence of this effect in the average over the entire orogen shows that it is not limited to a few locations.

In the following, we use $\overline{S}_A$ at a catchment size $A = \frac{1}{4}\,\mathrm{km}^2$, which belongs to the uppermost headwater regions and seems to be rather small compared to most studies on fluvial erosion (Wobus et al., 2006, and references therein). More precisely, we analyze all sites with A between $\frac{1}{16}\mathrm{km}^2$ and $1\,\mathrm{km}^2$. As an example, Fig. 3 illustrates the location of these sites in the upper Rhone Valley. Our choice is a trade-off between the amount of available data and being sure that fluvial processes dominate erosion. If A is too low, hill slope processes will dominate, so that the more or less continuous erosion may turn into threshold behavior. The uppermost curve in Fig. 2 illustrates this phenomenon as it seems to be limited by a mean slope value of about 0.55. In this case, the slope is no longer a proxy for the erosion rate. On the other hand, the number of available sites rapidly decreases with catchment size, so that the two lower curves show a strong variation at large elevations. Although their shape is essentially similar to the higher curves, the noise at high elevations make these large catchment sizes inappropriate for estimating erosion rates. According to these arguments, the similar shapes of the three solid curves in Fig. 2 suggest that the range from $A = \frac{1}{16}\,\mathrm{km}^2$ to $1\,\mathrm{km}^2$ is suitable for our analysis. This range covers almost one sixth of the total area of the Alps, while all larger channels contribute less than 4%. The nearly parallel course of the three solid curves suggests a logarithmic dependence of the erosion rate on catchment size, in contrast to a power law mostly assumed for larger catchment sizes. This rather weak dependence is included in the analysis, so that slopes can easily be recalibrated to $A = \frac{1}{4}\mathrm{km}^2$, although the data within the considered interval could be taken without recalibration as well.

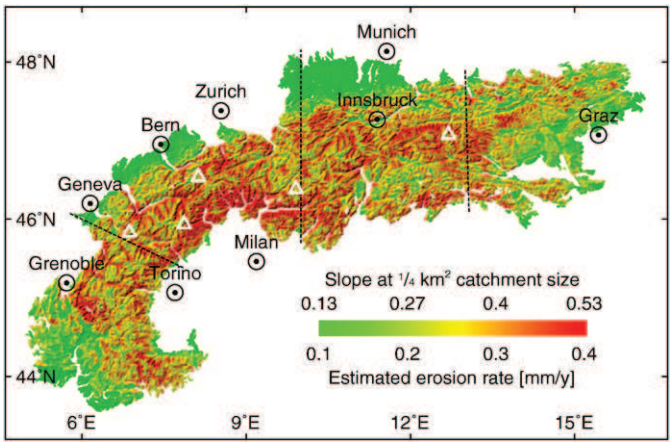

Fig. 1. Map of mean slope at $\frac{1}{4}\,\mathrm{km}^2$ catchment size of the Alps. The conversion of slopes to erosion rates is based on the sediment budget and is discussed later in the paper. White triangles represent the highest peaks of major massifs: Mont Blanc, Monte Rosa, Finsteraarhorn, Piz Bernina, and Groβglockner (from west to east). The separation by the dashed lines is related to Fig. 5.

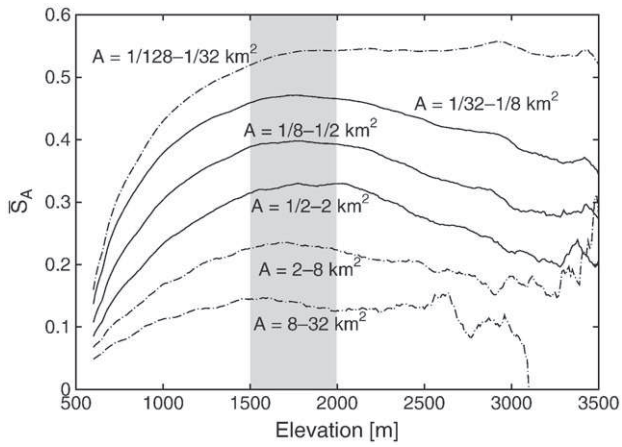

Fig. 2. Plot of $\overline{S}_A$-elevation relationships for various catchment sizes in the Alps. The gray field marks the range of elevation with the largest $\overline{S}_A$ values.

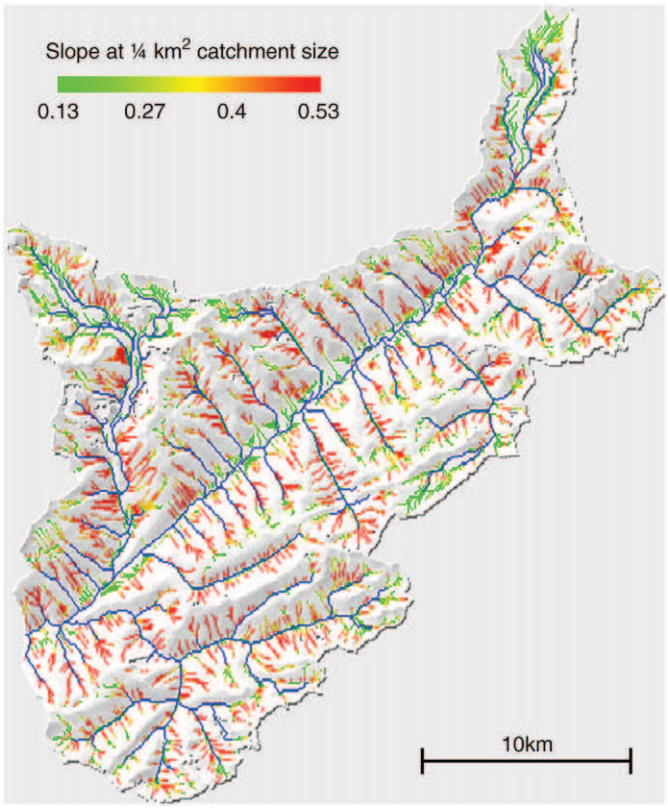

Fig. 3. Sites with catchment sizes from $A = \frac{1}{16}$ km^2 to 1 km^2 (colored according to their slope, rescaled to $A = \frac{1}{4}$ km^2 as discussed later in the text) and channels with $A > 1$ km^2 (blue) in the upper Rhone Valley.

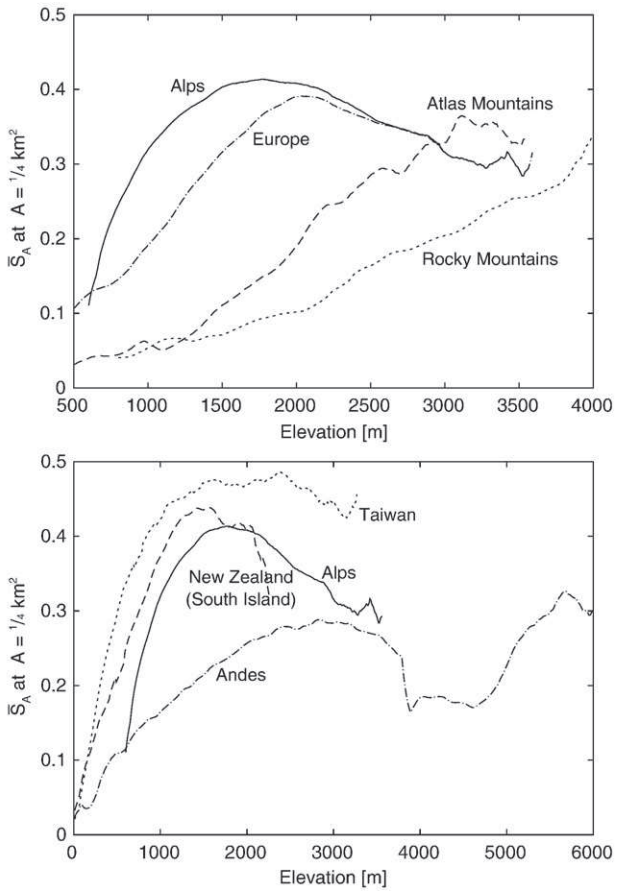

Fig. 4. The $\overline{S}_A$-elevation relationships of six mountain ranges.

The smoothed spatial distribution of $\overline{S}_A$ at $A = \frac{1}{4}$km^2 determines the surface color in Fig. 1. The decrease in $\overline{S}_A$ at high elevations is immediately visible in the map, too: The highest values occur not in the vicinity of the main crest, but rather north and south of it, and the regions around the highest mountains are characterized by moderate slopes. The corresponding $\overline{S}_A$-elevation curve is shown in Fig. 4. For comparison, the same analysis was performed for the Rocky Mountains, the Andes, the Atlas Mountains, Taiwan and the South Island of New Zealand. For all orogens, the entire range from the highest peak down to a given elevation was taken, except for the Rocky Mountains, where only the central part from 30° and 50° northern latitude without the Cascades was considered in order not to mix up too many different components. Beside the European Alps, only the Alps of New Zealand show the startling systematic decrease of $\overline{S}_A$ above a certain elevation identifying the Alps as a mountain range with very peculiar topographic characteristics. The $\overline{S}_A$-elevation curves of the Andes and Taiwan show some decrease or at least stagnation of $\overline{S}_A$ at high elevations, too, although not as clear as in the Alps. This will be discussed later.

Comparing the Alps with the Atlas Mountains and the Rocky Mountains in the upper part of Fig. 4 reveals another apparently striking difference: While the $\overline{S}_A$-elevation of the Alps is strongly concave even in its increasing part, that of the two other orogens is nearly linear or even slightly convex. However, this finding may not be as important as the decrease at high elevations since it may be a result of the overall shape of the orogen. While the Alps look like a more or less uniform, narrow mountain range, the Atlas Mountains and the Rocky Mountains are easily divisible into several distinct parts. In order to illustrate the effect, we have included an analysis of the entire European topography without Scandinavia (for simplicity, it is in fact the western part of Eurasia to 25° eastern longitude) in Fig. 4. Obviously, the superposition of several smaller orogens destroys the sharp increase of $\overline{S}_A$ at small elevations and results in a more or less straight curve. The decrease of $\overline{S}_A$ at high elevation of course persists since this elevation range is governed by the Alps.

In return, the Alps are not as homogeneous as their DEM suggests. So may the decrease of $\overline{S}_A$ be the result of a superposition of different regions which are not clearly distinguished in the DEM? In order to clarify this, we split up the Alps into the four regions separated by the dashed lines in Fig. 1. The parts are numbered I (south-west), II, III (the two central parts) and IV (east). Their $\overline{S}_A$-elevation relations shows a small, but rather unsystematic variation. The decrease of $\overline{S}_A$ is clearly visible in all parts except part IV where elevations in the

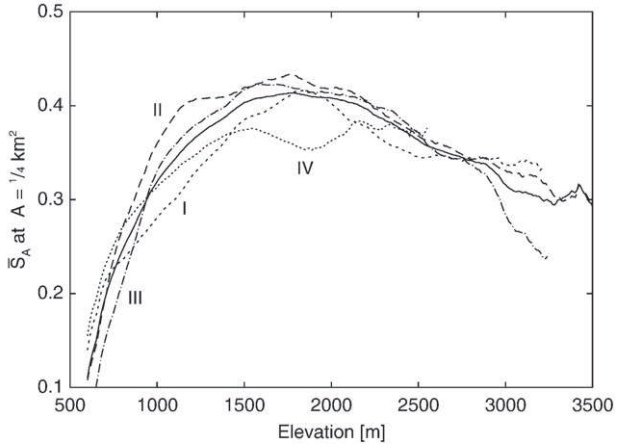

Fig. 5. The $\overline{S}_A$-elevation relationships of the Alps splitted into four parts.

interesting range become sparse although our method makes almost one sixth of all surface data usable. So the phenomenon originates from the entire Alps and is not the result of a superposition.

There are three possible interpretations of the decrease in $\overline{S}_A$ at high elevations in the entire Alps:

1. A systematic lithological, biological or climatological variation making rocks at high surface elevations more erodible, so that equilibrium is maintained by high erosion rates acting on less steep slopes.
2. A lack of uplift at high elevations, so that equilibrium can be maintained by low erosion rates.
3. Geomorphic disequilibrium where erosion has not yet balanced rock uplift at high elevations.

A systematic increase of erodibility with elevation due to rock lithology can be excluded because the highest parts of the Alps are generally characterized by high grade metamorphic rocks. The same applies to biological effects as soil-mantled slopes tend to be less steep than bedrock slopes (Montgomery, 2001) and climatic effects such as permafrost and orographic precipitation. So all these effects should rather support the increase of slopes with elevation than cause a systematic decrease. Furthermore, these effects should be visible in almost all mountain belts.

The second explanation – a lack of uplift at high elevations – was found for the Tibetan Plateau (Molnar and Lyon-Caen, 1989) and the Altiplano (Dalmayrac and Molnar, 1981). The sudden decrease of $\overline{S}_A$ above about 3500 m in the $\overline{S}_A$-elevation curve of the Andes (Fig. 4) in fact originates from the region around the Altiplano. However, for the Alps this idea is not consistent with measurements of recent uplift rates (Kahle, 1997; Ruess and Höggerl, 2002) as there is no systematic decrease of uplift rates at high elevations.

Since both concepts based on equilibrium fail to explain our observations, only the idea that regions above 1500-2000 m are not yet in geomorphic equilibrium remains: Erosion rates are smaller than rock uplift, so that these regions still experience a net increase in elevation (i.e. surface uplift). Further support for this idea might arise from a new study on cosmogenic nuclide-derived erosion rates (Norton et al., 2010b): While erosion apparently keeps track with rock uplift at moderate uplift rates up to about 1 mm/y, significantly lower denudation rates were found at some locations of high uplift.

But what is the signal causing the yet unfinished response of topography? It may originate from tectonics, but glaciation is a candidate, too. Even combinations seem to be possible since a part of the present uplift may be the isostatic response to deglaciation (Barletta et al., 2006; Champagnac et al., 2007). Glaciation itself obviously affects the topography, wide U-shaped valleys instead of rather narrow, V-shaped valleys are the most striking feature. However, U-shaped valleys are found at various elevations, and it may even depend on the total width of the valley whether the U-shape leads to an increase or a decrease in $\overline{S}_A$. Therefore, even some predominance of U-valleys at high elevation seems not to be able to explain the rather sharp transition from a strong increase of $\overline{S}_A$ to a decrease. Of course there may be an overall effect of glaciation. The Alps may have been much higher before glaciation and may have been torn down strongly during the glacial periods. However, this would imply that overall glacial erosion rates are significantly higher than fluvial erosion rates, while recent studies (Koppes and Montgomery, 2009) did not encounter a systematic difference between both.

However, response to deglaciation might have an effect on the analysis. As recognized by Norton et al. (2010a) in the upper Rhone Valley, the transition from glacial erosion to fluvial erosion may result in very high slopes locally, and these extremes might cause a bias in our analysis. Fig. 6 shows the cumulative distribution of slopes at three elevation slices. While the distributions are similar in total, the highest elevations are characterized by a weaker tail at very high

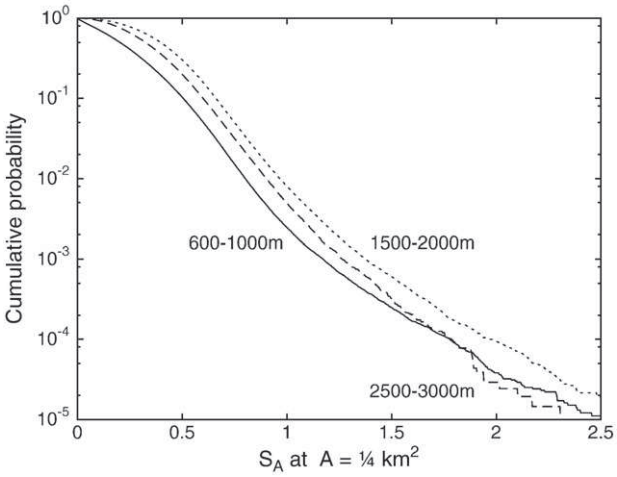

Fig. 6. Cumulative distribution of the slopes S_A at $A = \frac{1}{4}\,\mathrm{km}^2$ within three elevation slices.

slopes. Thus, very steep slopes occur less frequently at high elevations where the erosional response to deglaciation should in fact be weaker than at lower elevations. However, the effect of the very steep slopes on our analysis is negligible because all slopes $S_A > 1$ contribute less than 0.01 to the mean value $\overline{S}_A$ at all elevations. Thus, the erosional response to deglaciation can be detected by our method, but its effect causes no bias in our analysis. Moreover, the Rocky Mountains were partly glaciated, too, but exhibit a completely different $\overline{S}_A$-elevation than the Alps, while the Atlas Mountains were not glaciated and seem to be topographically similar to the Rocky Mountains. And finally, an analysis of a small, non-glaciated region at the edge of the Alps east of the Last Glacial Maximum (results not shown here) resulted in a similar $\overline{S}_A$-elevation relationship as for the entire Alps.

In sum, effects of glaciation on our analysis seem to be insignificant, so that an unfinished response to a tectonic signal remains as the most promising idea.

3. A Simple Model

The results of the previous section suggest that the highest regions of the Alps are not in geomorphic equilibrium and thus still grow. In order to test this hypothesis and to quantify their degree of maturity, we derive a simple, one-dimensional model for the evolution of a mountain belt. Compared to more elaborate models involving many parameters, the approach may even be oversimplified, and it seems to be impossible to justify the assumptions with regard to the Alps in detail. Justification will arise from its ability to reproduce and explain the observations.

In contrast to our analysis of the Alpine topography, an erosion model requires an explicit relationship between erosion rate, slope and catchment size. We thus come back to the stream power approach (e.g., Whipple and Tucker, 1999; Wobus et al., 2006). We assume that the erosion rate is proportional to the slope and increases with the distance from the main drainage divide raised to some power α. The power law exponent α summarizes the increase of erosion rate with the catchment size and the increase of catchment size with the distance from the drainage divide. We furthermore assume a "tent-shaped" uplift function corresponding to simple folding of a thin sheet according to compression, i.e., that the uplift rate linearly decreases from the main drainage divide to the margins of the mountain belt. Under these assumptions, uplift and erosion are described by a linear first-order differential equation of the hyperbolic type:

$$\frac{\partial}{\partial t}H(x,t) = \underbrace{U\left(1-\frac{x}{l}\right)}_{\text{uplift rate}} - \underbrace{\left(-Ex^{\alpha}\frac{\partial}{\partial x}H(x,t)\right)}_{\text{erosion rate } R(x,t)} \qquad (1)$$

for $0 \le x \le l$ where x is the coordinate perpendicular to the crest (the main drainage divide) and l is the distance from the crest to the margins. For symmetry reasons, we only consider one half of the mountain belt. The negative sign within the erosion rate $R(x,t)$ originates from the fact that $\frac{\partial}{\partial x}H(x,t)$ will become negative for our coordinate choice. Furthermore, U denotes the uplift rate at the crest, and E is a parameter that quantifies erodibility, precipitation, etc.

As shown in the Appendix A, Eq. (1) can be solved analytically starting from a flat surface $H(x,0)=0$. It is found that the surface reaches a steady state after the time $T = \frac{l^{1-\alpha}}{(1-\alpha)E}$, and that the maximum elevation (at the crest) finally becomes $H_{max} = \frac{l^{1-\alpha}U}{E(1-\alpha)(2-\alpha)}$. This result suggests nondimensional variables, i. e., to measure x in terms of l, t in terms of T, $H(x,t)$ in terms of H_{max}, and $R(x,t)$ in terms of U. With these nondimensional variables it is found that the region with $x \ge (1-t)^{\frac{1}{1-\alpha}}$ is in equilibrium at the time t, and

$$H(x,t) = (2-\alpha)\left(1-x^{1-\alpha}\right)-(1-\alpha)\left(1-x^{2-\alpha}\right) \quad (2)$$

$$R(x,t) = 1-x \quad (3)$$

In the region with $x < (1-t)^{\frac{1}{1-\alpha}}$, erosion does not keep track with uplift, resulting in an increase of elevation. We obtain:

$$H(x,t) = (2-\alpha)t-(1-\alpha)\left(\left(x^{1-\alpha}+t\right)^{\frac{2-\alpha}{1-\alpha}}-x^{2-\alpha}\right) \quad (4)$$

$$R(x,t) = \left(x^{1-\alpha}+t\right)^{\frac{1}{1-\alpha}}-x \quad (5)$$

Apart from the scaling parameters in the nondimensional variables, the power law exponent α is the only nontrivial model parameter.

Fig. 7 illustrates the behavior of the solution given by Eqs. (2)–(5). On the way to geomorphic equilibrium reached at $t=1$, the erosion rate has a maximum somewhere between the central divide and the margins. As uplift continues and the range equilibrates, the maximum moves towards the watershed and thus towards higher elevations. In the surface topography itself the transition point is reflected by a discontinuity in curvature which separates a quite linear part (in the upper reaches) from a more concave part (in the lower reaches). This change in curvature is not a "knickpoint" in the well-known sense, but still defines an important departure from an exponential equilibrium profile of a graded river bed. As this characteristic point of the stream morphology is barely noticeable in plots of longitudinal river profiles, its substantial implications for the erosion rate remained unnoticed before.

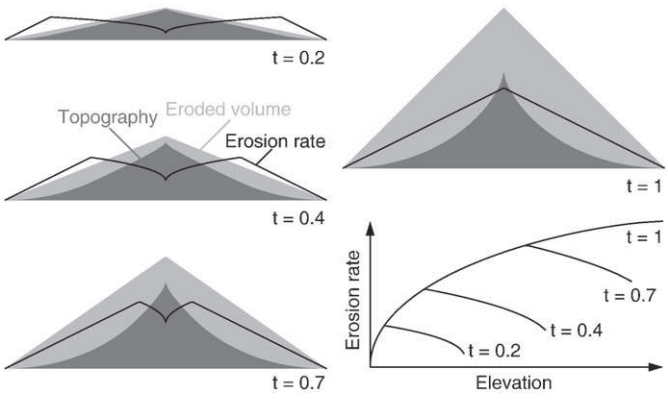

Fig. 7. Concept of the one-dimensional uplift/erosion model. The cartoons illustrate a mountain belt at four time steps approaching geomorphic equilibrium ($t=1$).

Excitingly, plotting erosion rates versus elevation for this simple model (Fig. 7) reproduces our findings from Fig. 4: A convex increase up to a certain elevation, and a slow decrease at higher elevations. The model reproduces the $\overline{S}_A$-elevation curves of the European Alps and the Alps of New Zealand at least qualitatively and indicates that both are far off from geomorphic equilibrium. Taiwan appears to be in or very close to equilibrium. Interpreting the curve of the Andes remains difficult, but the recovery of the slopes at high elevations points towards geomorphic equilibrium.

4. The State of Maturity of the Alps

The dashed line in Fig. 8 shows a visual fit of our model to the $\overline{S}_A$-elevation curve of the Alps. We found that the curvature in the left hand part, the position of the turnover at maximum $\overline{S}_A$, and the decrease to the right constrain the model parameters well. In contrast, the sharp bend at the point of maximum erosion rate is an artefact of the one-dimensional approximation because each elevation is assigned to only one location and thus to only one uplift rate here. In contrast, the same elevation occurs at many locations and thus at various uplift rates in reality. Thus, focus was laid on fitting the rest of the curve.

The visual fit results in a power law exponent $\alpha = \frac{1}{3}$ and a non-dimensional time $t=0.4$, which means that only 40% of the time towards geomorphic equilibrium has passed. Testing the fit with other parameters we found that the uncertainty of this value is lower than 0.1.

The combination of the excellent match between data and model for the Alps with the well constrained parameters allows a series of far reaching interpretations: The Alps are not even half way from a rather low (in the simple model completely flat) topography to their state of geomorphic equilibrium. While regions lower than 1500 m have already reached their final height, higher regions will still rise if the convergence between Adriatic plate and European plate continues. From the model results we can further derive that the net rise of the highest regions may amount to 2000 m. However, this number should be treated with caution as it hinges on the assumption that Pliocene and Quaternary rock uplift persists in the future. Furthermore, the gain in elevation may be limited by effects of slope instability above a critical slope. The $\overline{S}_A$-elevation curve floors at an elevation of 550 m: This suggests that the Alpine range is built on a base level of this elevation which is indeed close to the elevation of the Molasse basins.

The model also allows an estimate of the cumulative erosion during a hypothetic evolution of the topography from a nearly flat surface towards the present state. Maximum erosion amounts to about 900 m thickness and occurs at a present elevation of 1300 m.

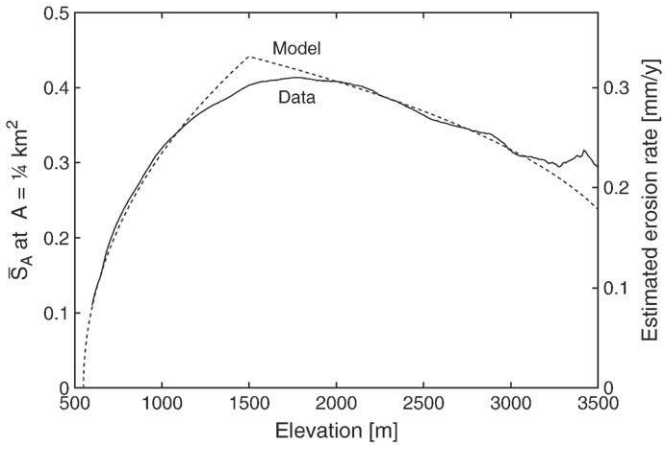

Fig. 8. Visual fit of the model result to the $\overline{S}_A$-elevation curve of the Alps. The scale of erosion rate is explained in Section 5.

This value decreases to 600 m at 3000 m elevation, which means that these regions should have experienced about five times more uplift than erosion so far. Such predictions are consistent with the observations that Miocene surfaces are largely preserved in several places (Hejl, 1997; Frisch et al., 2001; Dunkl and Frisch, 2002; Kuhlemann, 2007), but are inconsistent with mean erosion rates since the Miocene. We will take up this discussion after constraining the absolute time scale in the next section.

5. The Absolute Age of the Alpine Topography

As the time axis of our model can be arbitrarily rescaled, it does not allow any direct estimates of the absolute age of the topography. Combining the cumulative erosion with the hypsographic curve of the Alps leads to a total eroded volume of about 120,000 km^3, but this can in principle be distributed over an arbitrary time interval. However, recent uplift rates in the order of 1 mm/y found in high regions (Kahle, 1997) give a first hint: If these rates are representative during the formation of topography and only a few hundred meters were lost by erosion, the whole process cannot have taken more than a few million years.

Quantitative data on the sediment budget of the Alps (Kuhlemann et al., 2002; Kuhlemann, 2007) allow a more precise estimate. The observed sediment data (crosses in Fig. 9) show only one strong, continuous increase through time, beginning 5-6 my ago. Although climatic effects have been suggested as a cause for this (Cederbom et al., 2004; Willett et al., 2006), no consistent explanation has been found for this increase so far. Indeed, it has been argued (Molnar, 2004) that, even if the global sudden increase of erosion in the late Cenozoic is related to climatic effects it remains questionable how it did so. Our model predicts a nearly linear increase of sediment yield per time from beginning of topography build up to the present state. Therefore, we argue here that – for the European Alps – these 5-6 my relate to the onset of considerable topography build up and corresponds to the 40% of time towards morphological equilibrium. Then another 8-9 my are required for the Alps to reach a geomorphic steady state, and the increase in sediment yield shall strongly decelerate in future, as is shown in the trend of the modeled curve in Fig. 9.

In order to test this hypothesis we have calculated the sediment volumes predicted by our model, and plotted them as the solid line in Fig. 9. The modeled curve is shifted to a base level of 25,000 km^3/my (dashed line), assuming a more or less constant background sedimentation rate throughout the Miocene. It may be seen that the sediment yield predicted by the model (grey area corresponding to 120,000 km^3, representing the nondimensional time $t=0.4$) is even slightly lower than the amount of sediment found in nature. In other words, the sediment found in nature is enough to capture the volume lost by erosion during topography build up. This result clearly supports our hypothesis that the formation of the present Alpine topography (at least of major parts) started only 5-6 my ago. This correlates well to the onset of uplift in the Molasse basins (Genser et al., 2007), so that the formation of the Alpine topography and the uplift of the Molasse basins may be more related to each other than previously assumed.

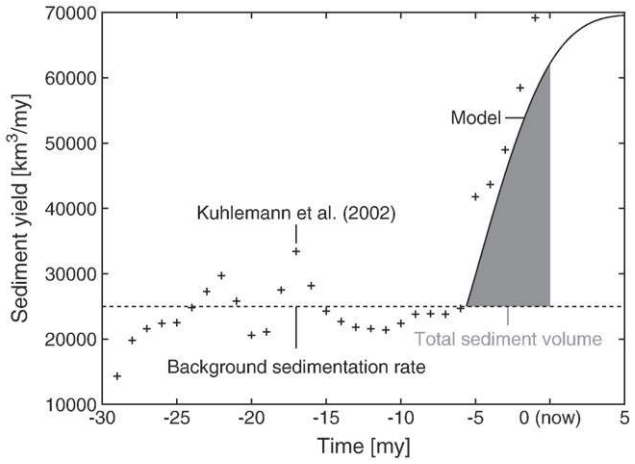

Fig. 9. Predicted sediment yield of the model (continuous line) in comparison with the sediment yield data for the Alps (crosses) (Kuhlemann et al., 2002). The dashed line represents the background sedimentation rate throughout the Miocene; the gray area represents the nondimensional time $t=0.4$ up to present.

Finally, constraining the time scale through the sediment budget allows the translation of $\bar{S}_A$ to erosion rates as anticipated in Figs. 1 and 8: Under the lithologic and climatic conditions of the Alps, erosion rate in millimeters per year is roughly three quarters of the slope at a catchment size of $\frac{1}{4}$km^2.

6. Limitations of the Model

We now come back to the circumstance that we used a perhaps oversimplified model. The one-dimensional approach itself is a very crude approximation, and the time-independent, tent-shaped uplift function may be qualitatively reasonable, but the real uplift pattern of the Alps is much more complex. Furthermore, effects of isostasy, perhaps in combination with lithospheric flexure, are disregarded. However, the main result concerning the equilibrium topography is an increase of erosion rate with elevation, and this hinges on an increase of uplift rate with elevation, but not on mapping this increase on a spatial pattern in detail. Both the curvature of the rising branch in Fig. 8 and the shape of the curve around the maximum may of course depend in detail on the spatial pattern, but the general result on disequilibrium does not.

Isostatic adjustment as the result of deglaciation or redistribution of sediment may in reality result in a time-dependent uplift rate. However, the main effect would be a non-linear timescale, which means that the transfer from the non-dimensional model time to the real time scale is not constant through time. This obviously affects the shape of the increase in sediment yield starting at 5-6 my b.p., which is indeed not reproduced perfectly. However, the point of onset itself should not be affected.

Therefore, the limitations of the perhaps oversimplified realization of our model approach should neither affect our results on the state of maturity nor on the absolute age of topography.

7. Earlier Topography

In Section 5 we found that building up the Alps from a base of 550 m elevation during the last 5-6 my reproduces the present topographic characteristics and the observed increase in sediment yield very well. However, we shall not conclude that the Alps were just a hilly flat throughout the Miocene. This would obviously contradict to measured exhumation rates as well as to the mean Miocene sediment delivery of about 25,000 km^3/my (dashed line in Fig. 9). Although opening and filling of basins lead to huge redistribution of sediment, this seems to be impossible without any topography.

Our analysis does not enable us to reconstruct the Miocene topography. But if we assume that it was close to geomorphic equilibrium and from its overall structure similar to the present topography, we can make a rough and, of course, speculative estimate. From the simple model we first estimate the increase of elevations towards geomorphic equilibrium and compute the corresponding hypsographic curve. As Fig. 10 illustrates, regions above 2000 m elevation will significantly rise if uplift persists. Since sediment yield is about 70,000 km^3/my in equilibrium (asymptotic behavior in Fig. 9), we then rescale the equilibrium state (relative to a base of 550 m) by a

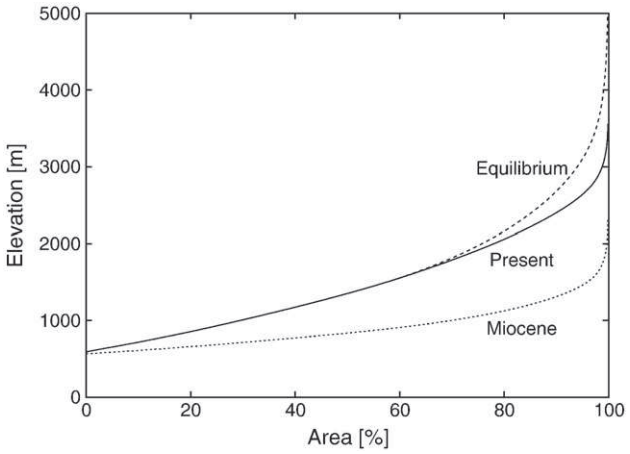

Fig. 10. Hypsographic curves of the Alps: Present, estimated for geomorphic equilibrium, and downscaled according to the Miocene sediment yield.

factor 25,000/70,000 to obtain an estimate of the Miocene hypsographic curve. The result shown in Fig. 10 suggests that only 4% of the area might have been above 1500 m in Miocene, compared to more than 40% today.

As a consequence of geomorphic equilibrium, the estimated hypsographic curve of the Miocene is relatively steeper in the upper part compared to the present. Although this is only a guess, it fits well to the idea that Miocene topography was more dissected than the present (e.g. Fitzsimons and Veit, 2001).

8. Conclusions

Our analysis of the Alpine topography in combination with a simple model of uplift and erosion gives strong evidence that the Alpine topography is still in its infancy and far off from geomorphic equilibrium. Comparing our results with sediment budget data leads to the conclusion that the formation of the present topography began only 5-6 million years ago at the end of the Messinian. Miocene topography should have been much lower and/or more dissected than the present topography. A clear difference between the topographic evolution of the Western and Eastern Alps was not found.

These findings question the apparent consensus that the topographic evolution was distributed over much of the Miocene. A thorough discussion of these results in relation to existing knowledge on paleo-elevations will have to follow.

In return, "rewriting" the topographic history of the Alps might give new impulses to the reconstruction of paleoclimate in Central Europe.

Admittedly, this large-scale analysis does neither put any serious constraints on the shape of the Miocene topography nor explain why topography was formed or reshaped at the end of the Messinian. Ceasing of lateral extrusion may be a candidate for an explanation. More detailed studies of the present topography will show whether the slight and so far not very systematic differences found between western and eastern parts help us to understand these phenomena.

Acknowledgements

The authors thank the TOPO-ALPS group for discussions and the ESF project TOPO-ALPS for funding.

Appendix A. Mathematical Background

Our model of uplift and erosion is described by Eq. (1) for $0 \le x \le l$ with the initial condition $H(x,0)=0$. This linear hyperbolic differential equation can be solved analytically using the method of characteristic curves.

In a first step, we rescale x to a nondimensional coordinate $\hat{x} = \frac{x}{l}$, which transforms Eq. (1) to

$$\frac{\partial}{\partial t}H(\hat{x},t) = U[1-\hat{x}]_+ + \hat{E}\,\hat{x}^{\alpha}\frac{\partial}{\partial \hat{x}}H(\hat{x},t) \tag{A.1}$$

where $\hat{E} = \frac{E}{l^{1-\alpha}}$, and $[\ldots]_+$ denotes the positive part of its argument, so that $[1-\hat{x}]_+ = 1-\hat{x}$ if $\hat{x} \le 1$ and 0 else. This is introduced to allow values $\hat{x} > 1$. In the following, we omit the hats for convenience.

The characteristic curves of Eq. (A.1) are given by the equation

$$\frac{d}{dt}x(t) = -Ex(t)^{\alpha}. \tag{A.2}$$

Its solution is

$$x(t) = \left(x(0)^{1-\alpha} - (1-\alpha)Et\right)^{\frac{1}{1-\alpha}} \tag{A.3}$$

so that

$$\frac{d}{dt}H(x(t),t) = \frac{\partial}{\partial x}H(x(t),t)\frac{d}{dt}x(t) + \frac{\partial}{\partial t}H(x,t) \tag{A.4}$$

$$= U[1-x(t)]_+ \tag{A.5}$$

$$= \left[1-\left(x(0)^{1-\alpha} - (1-\alpha)Et\right)^{\frac{1}{1-\alpha}}\right]_+ \tag{A.6}$$

Starting from a flat surface at $t=0$, $H(x,0)=0$, integrating this result leads to

$$H(x(t),t) = U\int_0^t \left[1-\left(x(0)^{1-\alpha} - (1-\alpha)E\tau\right)^{\frac{1}{1-\alpha}}\right]_+ d\tau \tag{A.7}$$

$$= U\int_0^t \left[1-\left(x(t)^{1-\alpha} + (1-\alpha)Et - (1-\alpha)E\tau\right)^{\frac{1}{1-\alpha}}\right]_+ d\tau \tag{A.8}$$

and thus

$$H(x,t) = U\int_0^t \left[1-\left(x^{1-\alpha} + (1-\alpha)E(t-\tau)\right)^{\frac{1}{1-\alpha}}\right]_+ d\tau \tag{A.9}$$

$$= \frac{U}{E(1-\alpha)}\int_{x^{1-\alpha}}^{\min\{1,x^{1-\alpha}+(1-\alpha)Et\}} \left(1-\xi^{\frac{1}{1-\alpha}}\right)d\xi \tag{A.10}$$

$$= \frac{U}{E}\times\begin{cases} Et - \dfrac{\left(x^{1-\alpha}+(1-\alpha)Et\right)^{\frac{2-\alpha}{1-\alpha}} - x^{2-\alpha}}{2-\alpha} & \text{for } x < (1-(1-\alpha)Et)^{\frac{1}{1-\alpha}} \\ \dfrac{1-x^{1-\alpha}}{1-\alpha} - \dfrac{1-x^{2-\alpha}}{2-\alpha} & x \ge (1-(1-\alpha)Et)^{\frac{1}{1-\alpha}} \end{cases} \tag{A.11}$$

The lower expression is time-independent, which means that erosion balances uplift for $x \ge (1-(1-\alpha)Et)^{\frac{1}{1-\alpha}}$. The entire mountain belt has reached its steady state at the time $T = \frac{1}{(1-\alpha)E}$, and the elevation at the main drainage divide becomes

$$H_{max} = H(0,T) = \frac{U}{E(1-\alpha)(2-\alpha)} \tag{A.12}$$

Transforming Eq. (A.11) to the nondimensional variables $\frac{H}{H_{max}}$ and $\frac{t}{T}$ immediately leads to Eqs. (2) and (4). The rate of erosion (Eqs. 3 and 5) finally emerges from inserting this result into Eq. (1).

References

Barletta, V.R., Ferrari, C., Diolaiuti, G., Carnielli, T., Sabadini, R., Smiraglia, C., 2006. Glacier shrinkage and modeled uplift of the alps. Geophys. Res. Lett. 33, L14307.

Cederbom, C.E., Sinclair, H.D., Schlunegger, F., Rahn, M.K., 2004. Climate-induced rebound and exhumation of the European Alps model. Geology 32, 709–712.

Champagnac, J.D., Molnar, P., Anderson, R.S., Sue, C., Delacou, B.F., 2007. Quaternary erosion induced isostatic rebound in the Western Alps. Geology 35, 195–198.

Champagnac, J.D., Schlunegger, F., Norton, K., von Blanckenburg, F., Abbühl, L.M., Schwab, M., 2009. Erosion-driven uplift of the modern Central Alps. Tectonophysics 474, 236–249.

Dalmayrac, B., Molnar, P., 1981. Parallel thrust and normal faulting in peru and constraints on the state of stress. Earth Planet. Sci. Lett. 55, 473–481.

Dunkl, I., Frisch, W., 2002. Thermochronologic constraints on the Late Cenozoic exhumation along the Alpine and West Carpathian margins of the Pannonian basin. In: Cloething, S.A.P.L., Horváth, F., Bada, G., Lankreijer, A.C. (Eds.), Neotectonics and surface processes: the Pannonian Basin and Alpine/Carpathian System. : Stephan Mueller Special Publication Series, vol. 3. EGU, pp. 135–147.

Fitzsimons, S.J., Veit, H., 2001. Geology and geomorphology of the European Alps and the Southern Alps of New Zealand: A comparison. Mt. Res. Dev. 21, 340–349.

Frisch, W., Kuhlemann, J., Dunkl, I., Brügel, A., 1998. Palinspastic reconstruction and topographic evolution of the eastern alps during late tertiary tectonic extrusion. Tectonophysics 297, 1–15.

Frisch, W., Kuhlemann, J., Dunkl, I., Szekely, B., 2001. The dachstein paleosurface and the augenstein formation in the northern calcareous alps; a mosaic stone in the geomorphological evolution of the eastern alps. Int. J. Earth Sci. 90, 500–518.

Genser, J., Cloetingh, S.A.P.L., Neubauer, F., 2007. Late orogenic rebound and oblique Alpine convergence: New constraints from subsidence analysis of the Austrian Molasse basin. Global Planet. Change 58, 214–223.

Hay, W.W., Soeding, E., DeConto, R.M., Wold, C., 2002. The Late Cenozoic uplift – climate change paradox. Int. J. Earth Sci. 91, 746–774.

Hejl, E., 1997. 'cold spots' during the Cenozoic evolution of the Eastern Alps: Thermochronological interpretation of apatite fission-track data. Tectonophysics 272, 159–173.

Kahle, H.G., 1997. Recent crustal movements, geoid and density distribution: contribution from integrated satellite and terrestrial measurements. In: Pfiffner, O.A., Lehner, P., Heitzmann, P., Müller, S., Steck, A.S. (Eds.), Results of the National Research Program 20. Birkhäuser, Basel, pp. 251–259.

Kocsis, L., Vennemann, T.W., Fontignie, D., 2007. Migration of sharks into freshwater systems during the miocene and implications for alpine paleoelevation. Geology 35, 451–454.

Koppes, M.N., Montgomery, D.R., 2009. The relative efficacy of fluvial and glacial erosion over modern to orogenic timescales. Nat. Geosci. 2, 644–647.

Kuhlemann, J., 2007. Paleogeographic and paleotopographic evolution of the Swiss and Eastern Alps since the Oligocene. Global Planet. Change 58, 224–236.

Kuhlemann, J., Frisch, W., Dunkl, I., Szekely, B., 2001. Quantifying tectonic versus erosive denudation by the sediment budget; the Miocene core complexes of the Alps. Tectonophysics 330, 1–23.

Kuhlemann, J., Frisch, W., Szekely, B., Dunkl, I., Kazmer, M., 2002. Postcollisional sediment budget history of the Alps: Tectonic versus climatic control. Int. J. Earth Sci. 91, 818–837.

Kühni, A., Pfiffner, O.A., 2001. The relief of the Swiss Alps and adjacent areas and its relation to lithology and structure: topographic analysis from a 250-m DEM. Geomorphology 41, 285–307.

Luth, S.W., Willingshofer, E., 2008. Mapping of the post-collisional cooling history of the eastern alps. Swiss J. Geosci. 101 (Supplement 1), 207–223.

Molnar, P., 2004. Late Cenozoic increase in accumulation rates of terestrial sediment: How might climate change have affected erosion rates? Annu. Rev. Earth Planet. Sci. 32, 67–89.

Molnar, P., Lyon-Caen, H.D., 1989. Fault plane solutions of earthquakes and active tectonics of the Tibetan plateau and its margins. Geophys. J. R. Astron. Soc. 99, 123–135.

Montgomery, D.R., 2001. Slope distributions, hillslope thresholds and steady-state topography. Am. J. Sci. 301, 432–454.

Norton, K.P., Abbühl, L.M., Schlunegger, F., 2010. Glacial conditioning as an erosional driving force in the Central Alps. Geology 38, 655–658.

Norton, K.P., v. Blanckenburg, F., Kubik, P.W., 2010. Cosmogenic nuclide-derived rates of diffusive and episodic erosion in the glacially sculpted upper Rhone Valley, Swiss Alps. Earth Surf. Process. Land. 35, 651–662.

Robl, J., Hergarten, S., Stüwe, K., 2008. Morphological analysis of the drainage system in the Eastern Alps. Tectonophysics 460, 263–277.

Robl, J., Stüwe, K., Hergarten, S., 2008b. Channel profiles around Himalayan river anticlines: Constraints on their formation from digital elevation model analysis. Tectonics 27, TC3010.

Ruess, D., Höggerl, N., 2002. Bestimmung rezenter höhen- und schwereänderungen in österreich. In: Friedl, G., Genser, J., Handler, R., Neubauer, F., Steyrer, H.P. (Eds.), Pangeo Austria. Institut für Geologie und Paläontologie, Universität Salzburg, Salzburg, p. 151.

Schlunegger, F., Hinderer, M., 2001. Crustal uplift in the alps: Why the drainage pattern matters. Terra Nova 13, 425–432.

Stüwe, Barr, T.D., 1998. On uplift and exhumation during convergence. Tectonics 17, 80–88.

Vernon, A.J., van der Beek, P.A., T.Rahn, M.K., Sinclair, H.D., 2006. Quantifying latex Cenozoic denudation of the European Alps: Insights from a compilation of fission-track ages. Terra Nostra 2, 101.

Vernon, A.J., van der Beek, P.A., Sinclair, H.D., T.Rahn, M.K., 2008. Increase in late Neogene denudation of the European Alps confirmed by analysis of a fission-track thermochronology database. Earth. Planet. Sci. Lett. 270, 316–329.

von Blanckenburg, F., Wittmann, H., Kruesmann, T., Norton, K.P., Kubik, P.W., 2007. How fast do the Alps erode? a cosmogenic nuclide study on central Alpine river basins. Geochim. Cosmochim. Acta 71, A11073.

Whipple, K.X., Tucker, G.E., 1999. Dynamics of the stream power river incision model: Implications for height limits of mountain ranges, landscape response time scales and research needs. J. Geophys. Res. 104, 17661–17674.

Willett, S.D., Schlunegger, F., Picotti, V.I., 2006. Messinian climate change and erosional destruction of the Central European Alps. Geology 34, 613–616.

Wittmann, H., von Blanckenburg, F., Kruesmann, T., Norton, K.P., Kubik, P.W., 2007. Relation between rock uplift and denudation from cosmogenic nuclides in river sediment in the Central Alps of Switzerland. J. Geophys. Res. 112, 20.

Wobus, C., Wipple, K.X., Kirby, E., Snyder, N., Johnson, J., Spyropolon, K., Crosby, B., Sheehan, D., 2006. Tectonics from topography: Procedures, promise, and pitfalls. In: Willett, S.D., Hovius, N., Brandon, M.T., Fisher, D.M. (Eds.), Tectonics, Climate, and Landscape Evolution: Geological Society of America, pp. 55–74.